Inorganica Chimica Acta 557 (2023) 121679

Contents lists available at ScienceDirect

Inorganica Chimica Acta

journal homepage: www.elsevier.com/locate/ica

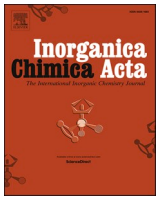

Adsorption structure of iron phthalocyanine and titanyl phthalocyanine on Cu(1 1 1)

Matthew A. Stoodley [a,b], Benedikt P. Klein [a,b], Michael Clarke [c], Leon B.S. Williams [a,d,e], Luke A. Rochford [f], Pilar Ferrer [a], David C. Grinter [a], Alex Saywell [c], David A. Duncan [a,*]

[a] Diamond Light Source, Harwell Science and Innovation Campus, Didcot OX11 0DE, United Kingdom
[b] Department of Chemistry, University of Warwick, Gibbet Hill Road, Coventry CV4 7AL, United Kingdom
[c] School of Physics and Astronomy, University of Nottingham, University Park, Nottingham NG7 2RD, United Kingdom
[d] School of Chemistry, University of Glasgow, University Avenue, Glasgow G12 8QQ, United Kingdom
[e] School of Physics and Astronomy, University of Glasgow, University Avenue, Glasgow G12 8QQ, United Kingdom
[f] Department of Earth Sciences, University of Cambridge, Downing Street, Cambridge, Cambridgeshire CB2 3EQ, United Kingdom

ARTICLE INFO

Keywords:
Quantitative structure determination
X-ray standing waves
Near-edge X-ray absorption fine structure
Synchrotron radiation
Soft X-ray photoelectron spectroscopy

ABSTRACT

The adsorption structure of iron phthalocyanine (FePc) and titanyl phthalocyanine (TiOPc) was studied by a combination of near edge X-ray absorption fine structure (NEXAFS) spectroscopy and normal incidence X-ray standing waves (NIXSW) technique. The FePc results demonstrate that the molecule adsorbs with the Fe metal centre at an adsorption height of 2.44 ± 0.09 Å, its macrocycle plane mostly parallel with the underlying surface and a single adsorption configuration. However, a small distortion of the isoindole groups, with respect to one another, is required to rationalise the results. The TiOPc results similarly indicate that the macrocycle plane is mostly parallel with the underlying surface up to thick multilayer films, yet, in the monolayer regime, the molecule must adsorb in multiple configurations. These configurations are nominally assigned to a mixture of adsorption configurations with some Ti=O bonds pointing towards the surface, and some pointing away. We determine that, in both configurations, the Ti metal centre sits at a similar adsorption height above the surface of 3.00 ± 0.20 Å.

1. Introduction

Tetrapyrroles are a popular class of organic semiconductor, both for their chemical stability and the ease of tuning their chemical properties by simply varying the species coordinated within the centre of the molecule. For example, first row transition metal or lanthanide centred tetrapyrroles are often employed for molecular magnetism applications [1–3]; specific centres can be used to treat certain types of cancer as photosensitisers for photodynamic therapy [4,5]; vanadyl phthalocyanine (VOPc) is paramagnetic [6], substituting the V for a Ti (titanyl phthalocyanine (TiOPc)) results in a diamagnetic molecule [7]. Distinctions can be drawn between planar and non-planar tetrapyrroles – those in which the central chemical species lies in plane with the ligand plane [8] and those where it projects above or below this plane [9]. Optical [10] and electronic [11] properties differ significantly between planar and non-planar tetrapyrroles and tuning of these properties is possible through chemical modification [12]. In addition, (and of direct relevance to this study) non-planar tetrapyrroles can exhibit multiple orientations ('upward' or 'downward' pointing, for example) in crystals, [13] thin films [14] and monolayers [15,16]. For many device applications these organic semiconductors must be interfaced with metallic contacts, e.g. copper, silver and gold. The relative energetic position of molecular orbitals and surface energy levels is of the utmost importance for efficient charge generation and extraction in electronic devices, especially at electrodes [17]. Thus, studying the interaction between these tetrapyrrole species and coinage metal surfaces is of particular interest, and has been the frequent focus of many studies [18–27].

Several structural studies have probed the conformation [28–33] and adsorption heights [16,34–43] of these molecules on the surface of Cu, Ag and Au, elucidating interactions between these molecular semiconductors and metallic supports. These adsorption heights, especially when measured quantitatively, are invaluable inputs and benchmarks for density functional theory (DFT) based calculations [37,44]. For the most part, these studies have yielded results that indicate comparatively

* Corresponding author.
E-mail address: david.duncan@diamond.ac.uk (D.A. Duncan).

https://doi.org/10.1016/j.ica.2023.121679
Received 21 March 2023; Received in revised form 8 June 2023; Accepted 7 July 2023
Available online 8 July 2023

simple "flat" adsorption (though, particularly for porphyrin tetrapyrroles, often with some distortion [32,45]), with the molecular plane of the tetrapyrrole macrocycle mostly parallel with the underlying substrate (with few exceptions [19,44]), and the molecule adsorbing with, primarily, just a single adsorption height. However, an exception to this has been the adsorption of non-planar phthalocyanines on the Cu(1 1 1) surface. Examples for the planar case include FePc (shown schematically in Fig. 1a) and CuPc; examples for the non-planar case are VOPc and TiOPc (shown schematically in Fig. 1b). While planar phthalocyanines have been observed to adsorb at a single adsorption height [36,39], with their molecular plane mostly parallel to the underlying surface, non-planar phthalocyanines appear to adsorb with two different orientations on the Cu(1 1 1) surface [16,42,46,47], with each orientation possessing significantly different adsorption height. Specifically, we have previously studied the adsorption structure of VOPc on Cu(1 1 1) [16] using normal incidence X-ray standing waves (NIXSW) [48]. The results of this previous study indicated that, regardless of coverage, the VOPc molecule adsorbs in a mixture of two primary orientations, broadly referred to as upwards and downwards pointing. Specifically, in the upwards configuration, the V=O bond has the oxygen atom further from the surface than the vanadium and *vice versa* in the downwards configuration, as shown schematically in Fig. 1c. The apparent change in molecular symmetry, often termed 'symmetry reduction' has been reported for planar [49] and non-planar [46] phthalocyanines on the Cu (1 1 1) surface. Unfortunately, these studies use mostly local probes such as scanning tunnelling microscopy (STM) which are difficult to quantify, and have not been directly correlated with a quantitative technique such as NIXSW.

Within the current work we present a structural study, employing both NIXSW and near edge X-ray absorption fine structure (NEXAFS) spectra to probe the adsorption structure and geometry of FePc and TiOPc on Cu(1 1 1). Our results reinforce the trend previously observed in the literature of a single adsorption height for the planar phthalocyanine, but two unique adsorption structures for the non-planar phthalocyanine. Furthermore, we can exclude the presence of a significant tilt (greater than 40°) of the molecular plane for either species, with respect to the surface plane, that has been suggested, for titanyl phthalocyanine, on other surfaces [50].

2. Experimental methods

Atomically clean Cu(1 1 1) surface of single crystals (SPL, Netherlands) were prepared by repeated cycles of sputtering (Ar^+, 1 keV) and annealing (~900 K). The cleanliness was assessed by soft X–ray photoelectron spectroscopy (SXPS). Both iron phthalocyanine (FePc – Fig. 1a) and titanyl phthalocyanine (TiOPc – Fig. 1b) were triply purified by thermal sublimation [51] before being loaded into an evaporation source for organic molecular beam epitaxy (OMBE). The evaporator contained two separately heated crucibles (OEZ 40-2x1-14-S, MBE Komponenten, Germany) that were water cooled to avoid inadvertent simultaneous evaporation of both molecules. To control the evaporation rate from the OMBE evaporator the FePc was sublimated at 650 K to grow a sub–monolayer or bilayer film; the TiOPc was sublimated at 630 K to grow a thick multilayer, 610 K to grow a trilayer and 550 K for a sub–monolayer film. Coverages are roughly estimated with respect to a saturated layer of pyrene on Cu(1 1 1) and comparison of the respective Cu 3s and C 1s intensities in the measured overview spectra. The coverage of the films associated with each figure is summarised in Table S1 in the electronic supplementary information (ESI).

The SXPS and NIXSW measurements were performed at the permanent end station of the I09 beam line (Diamond Light Source, UK) [52]. The I09 beam line consists of two separate undulator light sources that can simultaneously irradiate a sample with soft (0.11 to 2.00 keV) and hard (2.15 to 15.00 keV) X–ray light on the same spot on the sample. The end station has a Scienta EW4000 HAXPES analyser that was used to acquire the individual energy distribution curves in the NIXSW measurements, as well as the SXPS data. The analyser accepts a large range of emission angles (±28°) and was mounted perpendicular to the incidence direction of the photon in the plane of the photon polarization (linear horizontal). The SXPS measurements were acquired at an incidence angle of 70° and at photon energies of 900 eV (Fe 2p), 680 eV (O 1s and Ti 2p), 560 eV (N 1s) and 430 eV (C 1s). The NIXSW measurements were acquired at normal incidence to the (111) planes of the Cu surface, thus at normal incidence to the Cu(1 1 1) surface, with a Bragg energy of approximately $h\nu = 2.978$ keV. The $(1\bar{1}1)$ planes of the Cu surface are tilted by an angle of ~ 70° with respect to the surface, and NIXSW measurements from these reflection planes were also acquired at normal incidence to the plane at the same Bragg energy as the (111) measurements. Each individual NIXSW measurement was performed rapidly (~20 min) and multiple repeated measurements were acquired from different spots on the sample. On each individual spot the reflectivity curve was measured to ascertain the crystalline quality of that spot and allow exact energy alignment of the individual NIXSW measurements, which were summed to improve the signal-to-noise ratio. To measure the adsorption rate of the individual elements in the respective molecules, the photoemission rate from the core levels was monitored. For FePc, 3 Fe 2p, 2 N 1s and 3 C 1s NIXSW measurements were obtained from the (111) reflection, and 8 Fe 2p measurements from the $(\bar{1}11)$ reflection. For TiOPc, 7 Ti 2p, 2 N 1s, 3C 1s and 7 O1s NIXSW measurements were obtained from the (111) reflection. Non-dipolar effects in the angular dependence of the high-energy photoemission were corrected as described in ref. [48] using a value of the backward-forward asymmetry parameter, Q, [53] derived from the theoretical calculations of ref [54]. It was assumed that these non-dipolar effects in the measurements using a wide angular range of emission detection could be modelled by a mean value of the emission angle, θ, defined as the angle between the photon polarisation and the photoelectron detection direction. In all cases only emission at angles lying between the photon polarisation and the vector normal to the probed scatterer planes were used (i.e. values θ greater than 0 were included, θ less than 0 were excluded). For the $(\bar{1}11)$ reflection the Q parameter was calculated using a value of θ of 15°. For the (1 1 1) reflection the experimental geometry meant that the accepted angular range of the analyser included 90° grazing emission that is strongly attenuated so a slightly larger value of θ

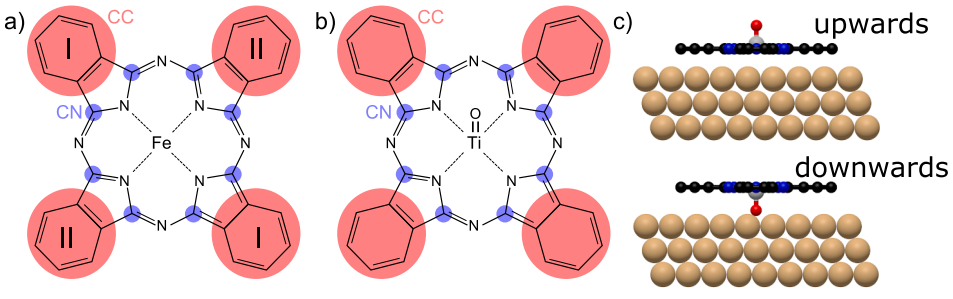

Fig. 1. Chemical structure of **a)** iron phthalocyanine (FePc) and **b)** titanyl phthalocyanine (TiOPc). The C atoms assigned to the CC (red) and CN (blue) species are highlighted with circles, the two pairs of isoindolic groups that are allowed to vary independently in the modelling are labelled with **I** and **II**. **c)** Schematic representation of the "upwards" and "downwards" configuration of vanadyl phthalocyanine (VOPc). Black spheres are C atoms, blue: N, red: O, grey: V, copper: Cu. (For interpretation of the references to colour in this figure legend, the reader is referred to the web version of this article.)

of 18° was used. The peaks present in the SXPS and the individual spectra of the NIXSW data were fitted with a convolution of a Doniach-Sunjic [55] and a Gaussian lineshape. A Gaussian error function was used to model the step under the spectra, and a straight line was used to fit the background.

The NEXAFS measurements were obtained from the permanent end station on the B-branch of the B07 beam line (Diamond Light Source, UK)[56,57] by Auger decay electron yield (AEY). The Auger decay electrons were detected using a SPECS Phoibos 150 hemispherical analyser that was mounted 60° away from the incident beam in the plane of the photon polarisation (linear horizontal). The NEXAFS data were normalized using the photocurrent measured off a positively-biased collector plate facing the final refocussing mirror on the beam line, which was assumed to be directly proportional to the incident photon flux. Spectra were also obtained over a similar photon energy range for a clean Cu(1 1 1) crystal, these spectra were similarly normalised to the mirror current. These "crystal" spectra were subtracted from the normalised NEXAFS data (apart from the thick TiOPc multilayer), to remove effects from the underlying substrate. From both the crystal spectra and the measured NEXAFS data, the signal between a binding energy of 0 and 10 eV were excluded, to mitigate the influence of the Cu valence band on the measurement. Prior to subtraction, the crystal spectra were rescaled such that the mean intensity in the pre-absorption edge region was the same as the normalised NEXAFS data. NEXAFS from the N K-edge ($h\nu = 390 - 450$ eV) and C K-edge ($h\nu = 280 - 350$ eV) were acquired at normal incidence ($\theta = 90^{\circ}$, where θ is the angle between the photon polarisation and the surface normal), magic angle ($\theta = 53^{\circ}$)[58] and grazing incidence ($\theta = 10^{\circ}$), to probe the orientation of the adsorbed molecules.

3. Results

3.1. Soft X-ray photoelectron spectroscopy (SXPS)

The SXP spectra for a submonolayer of both FePc and TiOPc on Cu (1 1 1) are shown in Fig. 2. We estimate that the coverage of these films are approximately 0.6 ML (where 1 ML is a densely packed monolayer of a molecular adsorbate), the overview spectra for these films are shown in the Figure S1 in the ESI. The C 1s SXP spectra (Fig. 2e) are similar for both species, showing two clearly separated peaks that are assigned, based on their relative binding energy, their relative intensity and the comparison to similar spectra in the literature [26,59], to carbon atoms only bound to other carbon atoms (CC, lower binding energy) and carbon atoms also bound to nitrogen atoms (CN, higher binding energy). The N 1s SXP spectra (Fig. 2d), in contrast, show subtle differences between the TiOPc and FePc layers. Namely the N 1s spectra corresponding to TiOPc seem to consist of a single, if somewhat broad, peak (as was observed for VOPc on the same surface [16]) suggesting that the chemical environment of all N atoms in the molecule are comparable. In contrast, the FePc monolayer shows a primary peak at a higher binding energy than the TiOPc, but a subtle shoulder at lower binding energies. A similar spectral shape was observed by Snezhkova et al. [26] and was ascribed to a 0.36 eV binding energy shift between the inner most N, coordinated to the central Fe atom, and the outer N atoms that link the isoindolic groups, rather than from the presence of a second FePc species on the surface. The Ti 2p (Fig. 2c) and Fe 2p (Fig. 2a) SXP spectra both show a single primary peak, with an associated splitting related to the spin–orbit coupling. In the Ti $2p_{3/2}$ spectrum, the peak is at a binding energy of 457.5 eV, which corresponds well to Ti(IV)[27], with a

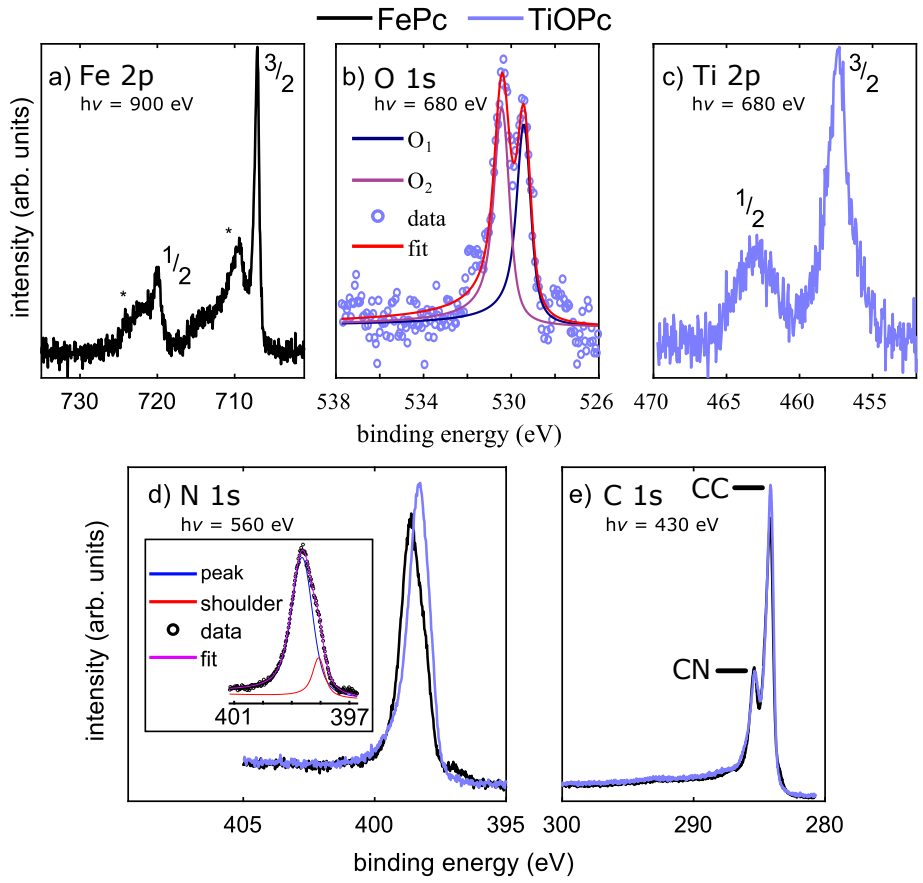

Fig. 2. Soft X-ray photoelectron spectroscopy (SXPS) of FePc and TiOPc on Cu(1 1 1). The peaks labelled CN and CC are assigned to the C atoms as indicated in Fig. 1a,b. The inset in panel d) presents an illustrative fitting of the N 1s spectra of FePc on Cu(1 1 1), highlighting the presence of a shoulder next to the main peak. The $\frac{3}{2}$ and $\frac{1}{2}$ spin orbit components of the (a) Fe 2p and (c) Ti 2p spectra are highlighted. The loss feature in the (a) Fe 2p spectrum is indicated with by an asterisk (*).

possible shoulder at lower binding energy that may suggest a minority Ti (III) species, possible TiPc or TiOHPc. The Fe $2p_{3/2}$ spectrum exhibits a significant feature at ~ 710 eV that is assigned to a loss feature related to the coupling of the core hole with unpaired electrons in the Fe valence band [60], as is commonly observed in Fe 2p spectra [37,60,61]. The O 1s SXP spectrum (Fig. 2b) of TiOPc shows two unique peaks that are labelled as O_1 (lower binding energy) and O_2 (higher binding energy) which, as is discussed below, are loosely assigned to the O atoms that are above or below the *Pc* molecular plane.

3.2. Normal incidence X-ray standing waves (NIXSW)

The NIXSW technique [48] exploits the X-ray standing wave that is created by the interference between the incident and reflected waves close to the Bragg condition for a given Bragg reflection $H = (h,k,l)$. The period of this standing wave matches the interplanar spacing d_H between the Bragg diffraction planes. In the case of a homoatomic, face centred cubic crystal structure (e.g. pure Cu) the Bragg diffraction planes are coincident with the atomic planes. The phase of the standing wave, and thus the location of the maximum intensity of the standing wave with respect to the Bragg diffraction planes, varies when the photon energy is scanned through the Bragg condition. When the phase is zero, the maximum intensity lies halfway between Bragg diffraction planes; when the phase is π the maximum intensity is coincident with the Bragg diffraction planes [62]. Any atom immersed in this standing wavefield will experience a varying electromagnetic field intensity as a function of its position between these diffraction planes, resulting in a characteristic absorption profile, which can be acquired by monitoring the photoelectron intensity profile. The measured profile is then fitted uniquely, using dynamical diffraction theory [63], by two dimensionless parameters [48]: the coherent fraction, f_H, and the coherent position, p_H. These are, respectively, the amplitude and phase of a Fourier transform component of the absorber location and broadly correspond to the degree of order and the mean position, respectively, of the absorber atoms relative to the Bragg diffraction planes. By recording NIXSW data at different Bragg reflections, we can use these amplitude and phase values to triangulate the position of the emitter atoms with respect to the underlying bulk crystal. [48] When the chosen Bragg diffraction plane is parallel with the surface plane the coherent position is related to the mean adsorption height of a species by:

$$h_H = (n + p_H) \bullet d_H \quad (1)$$

where n is an integer, and relates to so called "modulo-d" ambiguity [64] where adsorption heights that differ by the interplanar spacing cannot be directly differentiated. However, in practice the correct value of n can often be easily assigned as d_H typically is in the order of ~ 2 Å, thus it is generally trivial to exclude adsorption heights that are unphysically low or high.

The NIXSW data arising from the (1 1 1) reflection of the Cu substrate are shown in Fig. 3 for both molecules (unless otherwise indicated) from the C 1s, N 1s, Fe 2p (FePc), Ti 2p (TiOPc) and O 1s (TiOPc) region. The NIXSW from the $(1\bar{1}1)$ reflection for the Fe 2p region is shown in Figure S2 in the ESI. Note that the C 1s data were separately fitted for the CC and CN species, but the O 1s data were integrated across both species. The corresponding coherent fraction and coherent position, as well as the associated mean adsorption heights, for all species are shown in Table 1. Both the Fe 2p and Ti 2p region exhibit comparably large coherent fractions (0.78 ± 0.10 and 0.95 ± 0.25, respectively), that would generally be associated with a single adsorption height [65].

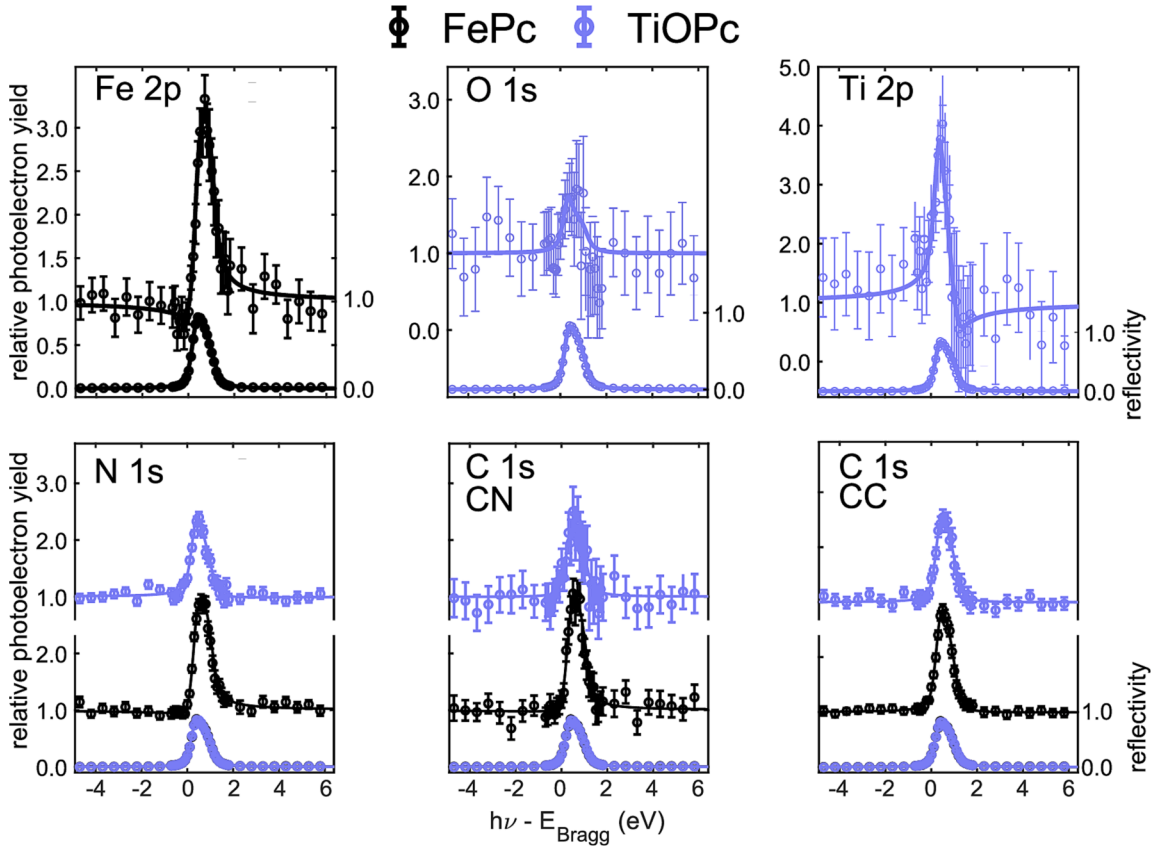

Fig. 3. The (111) NIXSW of a submonolayer of FePc on Cu(1 1 1) and a submonolayer of TiOPc on Cu(1 1 1). The resulting coherent fraction (f_{111}) and coherent position (p_{111}) from the shown fits are detailed in Table 1. The assignment of CN and CC in the SXPS is shown in Fig. 2, and the atoms to which they are assigned are shown in Fig. 1a,b. Relative photoelectron yield is the measured photoelectron intensity at the given photon energy related to that measured away from the Bragg condition (off-Bragg).

Table 1
Coherent fractions (f_H) and coherent positions (p_H) for the $H = (111)$ and $H = (1\bar{1}1)$ reflections from the fitting of the NIXSW spectra shown in Fig. 3 and Figure S2 (respectively). The numbers in brackets are the uncertainty in the last decimal place of the quoted values. The saddle shape model and offset model are shown schematically in Fig. 6 and are described in the main text. The atoms that are assigned to CC and CN are shown in Fig. 1a,b. The calculated adsorption heights, h_{111}, values are only shown for species with a coherent fraction greater than 0.7, and are calculated assuming a (111) d-spacing of 2.0871 Å.

	TiOPc/Cu(1 1 1)		FePc/Cu(1 1 1)		saddle shape model		offset model	
	f_{111}	p_{111}	f_{111}	p_{111}	f_{111}	p_{111}	f_{111}	p_{111}
CC	0.26(6)	0.29(5)	0.40(4)	0.30 (2)	0.42	0.28	0.41	0.31
CN	0.10 (13)	0.23 (17)	0.56 (10)	0.23 (5)	0.63	0.25	0.54	0.26
N	0.17(6)	0.38(6)	0.57(6)	0.20 (3)	0.50	0.21	0.69	0.22
Ti/ Fe	0.96 (25)	0.44 (10)	0.78 (10)	0.17 (4)	–	–	–	–
O	0.20 (20)	0.76 (20)	–	–	50/50 mixture of HCP/FCC site			
	$f_{1\bar{1}1}$	$p_{1\bar{1}1}$	$f_{1\bar{1}1}$	$p_{1\bar{1}1}$	$f_{1\bar{1}1}$		$p_{1\bar{1}1}$	
Fe	–	–	0.41(8)	0.95 (5)	0.39		0.89	
	h_{111}(Å)		h_{111}(Å)					
Ti/ Fe	3.00(20)		2.44(9)					

However, the coherent position found for the metal centres differs significantly, with the Ti metal centres found to adsorb 0.56 ± 0.23 Å higher than the Fe metal centres (see Table 1). For the N 1s and the two C species, for both FePc and TiOPc, the coherent fraction is significantly smaller than that found for the metal centres. This decrease is particularly notable in the TiOPc data, where the coherent fraction has almost been reduced to zero. Additionally, the O 1s TiOPc data also results in a similarly low coherent fraction. This result, taken by itself, would often be interpreted as an almost random height distribution of the phthalocyanine macrocycle. However, these two general assumptions, that the Ti metal centres occupy a single well defined adsorption height, yet that the molecular macrocycle and O atoms occupy an almost completely disordered, are clearly at odds with one another, and would instead indicate multiple discrete adsorption sites for the molecule, as was the conclusion in our prior work on VOPc on the same surface. The implications of this conclusion are discussed in detail below.

The high coherent fraction of the Fe, in the (111) data, and the comparably lower, but non-zero, coherent fractions of the C and N species, suggests that the FePc molecule is, in one way or another, distorted on the surface (with respect to the planar macrocycle exhibited in the single crystal structure [51,66]). The structure in the previously published DFT calculations of Snezhkova et al. [26] would result in a coherent fraction of greater than 0.95 (ignoring thermal vibrations) for all species, thus any distortions in the macrocycle must be larger than those predicted by Snezhkova et al.. The simplest possible distortion is a rigid tilt of the macrocycle with respect to the surface plane, however any significant tilt of the molecule is excluded by the NEXAFS in the following section. Furthermore, such a rigid tilt would result in the coherent fraction of the CC species being significantly smaller than that of the CN or N species. For example, for a comparatively small tilt of 10°, the coherent fraction of the CN and N species would be approximately 0.5, however the CC species would have a coherent fraction of 0.0. Simply tilting each of the isoindolic groups uniformly to maintain a C_{4v} point group also cannot explain the experimental results as all 8 atoms of the C—N species are all nearly equidistant from the metal centre. Thus, any possible uniform tilt of the isoindolic groups would still result in a high coherent fraction for this species. Thus, there are two other simple models that could be considered likely for distortion of the macrocycle. Specifically, a saddle shape conformation, where two of the isoindolic/pyrrole rings are tilted away from the surface and two are tilted towards it, or a static displacement of the isoindolic/pyrrole rings away from the surface. Saddle shapes have not been attributed to adsorbed phthalocyanines, but are commonly attributed to the more flexible porphyrin species on various surfaces, with an extreme version having been observed for free-base tetraphenyl porphyrin [19,44,45], but several recent structural studies into porphine, the simplest porphyrin, have suggested static displacement of the pyrrole rings [38,67,68]. Indeed, previously published DFT calculations for FePc on Cu(1 1 1) [20,26], suggest just such a static displacement, with only a moderate tilting. To probe the scale of any possible tilt in the adsorbed molecule, we performed C and N K-edge NEXAFS, described in the following section.

In the low coverage regime that the NIXSW measurements were obtained from, the FePc would be expected to be adsorbed in an isolated state with a well defined adsorption site, as indicated by prior STM measurements. [49,69] The $(1\bar{1}1)$ data from the Fe 2p region provides insight into this well defined site of the Fe metal centres. If the Fe metal centre were found in an atop, HCP or FCC site then the coherent fraction of the $(1\bar{1}1)$ data ($f_{1\bar{1}1}$) should be equal to that of the (111) data (f_{111}). If the metal centre were in a bridging site on the surface, as indicated in the work of Snezhkova et al. [49], then the $f_{1\bar{1}1}$: f_{111} ratio should be $\frac{1}{3}$: 1. Yet, instead, the $f_{1\bar{1}1}$: f_{111} was found to be almost 0.5:1 ratio. This is indicative of adsorption in a mixture of any two of atop, HCP and FCC sites. The $(1\bar{1}1)$ coherent position ($p_{1\bar{1}1}$) for such a mixture of sites for a HCP/atop ($p_{1\bar{1}1}^{HCP/atop}$), FCC/atop ($p_{1\bar{1}1}^{FCC/atop}$) and HCP/FCC ($p_{1\bar{1}1}^{HCP/FCC}$) mixture is:

$$p_{1\bar{1}1}^{HCP/atop} = \frac{n + p_{111}}{3} + \frac{1}{6} \quad (2)$$

$$p_{1\bar{1}1}^{FCC/atop} = \frac{n + p_{111}}{3} + \frac{1}{3} \quad (3)$$

$$p_{1\bar{1}1}^{HCP/FCC} = \frac{n + p_{111}}{3} + \frac{1}{2} \quad (4)$$

If $n = 1$ is assumed, which would correspond to a reasonable adsorption height of 2.44 Å, then $p_{1\bar{1}1}^{HCP/FCC}$ would be 0.89. This coherent position would be in good agreement with the experimentally measured $p_{1\bar{1}1}$ of 0.95 ± 0.05. Thus, in the measured coverage regime, if the Fe atoms are in high symmetry sites, that site is likely a mixture of FCC and HCP sites.

3.3. Near edge X-ray absorption fine structure (NEXAFS)

C and N K-edge NEXAFS data from a bilayer (~2.2 ML) of FePc on Cu (1 1 1) are shown in Fig. 4. The spectra show a clear dichroism, where the π^* region is most intense when the photon polarisation is mostly parallel to the surface normal ($\theta = 10^\circ$, grazing incidence, GI), but is almost completely suppressed when the photon polarisation is parallel to the surface plane/perpendicular to the surface normal ($\theta = 90^\circ$, normal incidence, NI). This indicates that the macrocycles of the adsorbed FePc molecules are predominantly parallel to the surface plane. For the N K-edge NEXAFS, comparing the intensity at a photon energy of 400.4 eV (the position of the maximum absorption rate for $\theta = 10^\circ$), the ratio of intensity between GI: magic angle ($\theta = 53^\circ$, MA): NI is 15: 5.5: 1. Assuming a photon polarisation of 90%, the GI:MA ratio would suggest a tilt of ~ 0°, whereas the GI:NI ratio would suggest a tilt of ~ 20°. Such a large discrepancy is to be expected, the comparatively small intensity in the NI signal will have a comparatively large associated uncertainty, as any errors present in the data correction and normalisation process will significantly affect the resulting intensity in this dataset. Furthermore, the remaining intensity of in the normal incidence spectra may simply result from disordered areas on the surface, especially in the second layer, or from hybridisation between the molecular orbitals and the surface states, as have been previously observed for porphyrins on the

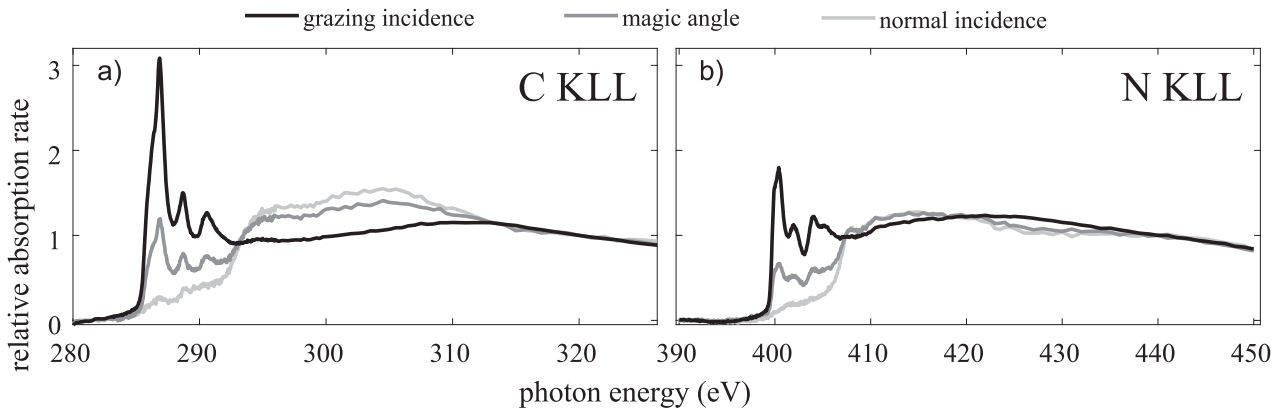

Fig. 4. (a) C KLL and (b) N KLL NEXAFS of a bilayer of FePc on Cu(1 1 1) as a function of the incidence angle. Note that the signal in normal incidence is almost, but not entirely, extinguished indicating that the molecular macrocycle must be adsorbed almost parallel to the surface plane.

same surface (e.g. [70]). However, these rough results do indicate that any expected tilt in the FePc macrocycle would be ~ 20° or less.

C and N K-edge NEXAFS data for a thick multilayer (no observable Cu substrate signal in the XPS) and a trilayer (~3.4 ML) of TiOPc on Cu (1 1 1) are shown in Fig. 5. Similar to the FePc bilayer data, these spectra indicate that the macrocycle of the TiOPc is largely parallel to surface plane at both film thicknesses, excluding any significant tilt of the molecule on the surface, such as that proposed by Wei et al. for TiOPc on Ag(1 1 1)[71]. Indeed, there is no indication of any significant amount of tilted TiOPc on the surface. The GI: MA: NI ratio at 400 eV for the thick and thin films were both found to be 12: 5: 1, which would suggest a molecular tilt of ~ 20°. The C KLL and N KLL of the thinner films (TiOPc and FePc) exhibit features that are broader than that observed for the thick multilayer (TiOPc). This may be due to hybridisation of the molecular orbitals with the underlying Cu substrate, in which case the hybridisation is more pronounced for the FePc film than the TiOPc film. The N KLL NEXAFS of the thick multilayer film of TiOPc agrees well with similar spectra from multilayers of FePc and AlClPc in the literature [72,73].

3.4. Model structures

To understand the results of the NIXSW and the NEXAFS measurements we performed some simple geometric modelling of possible adsorption configurations. This modelling is based upon distortions to the molecular macrocycle that have either been predicted by DFT calculations for phthalocyanines, [26] or have been observed for porphyrins, [74] adsorbed on metal surfaces. We rigidly distorted the molecule by varying three parameters: tilt of the isoindolic groups labelled **I** in Fig. 1a, tilt of isoindolic groups labelled **II** in Fig. 1a, and varying the relative adsorption height of groups **I** and **II**. The centre of rotation for the tilt was the lateral position of the Fe metal centre at the experimentally measured height of the N atoms, and the variation in relative adsorption height was also centred around the experimentally measured

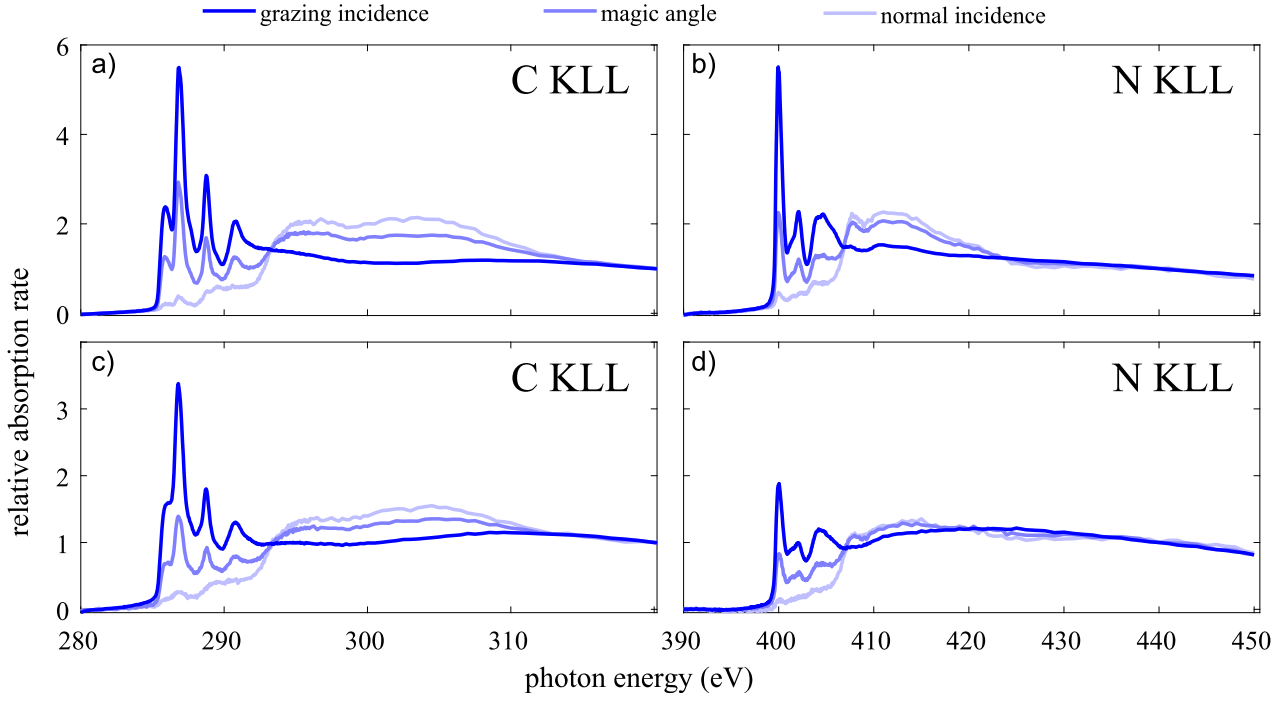

Fig. 5. (a,c) C KLL and (b,d) N KLL NEXAFS of a (a,b) thick (i.e. no observable substrate peaks in the SXPS, see Figure S1 in the ESI) and a (c,d) thin (i.e. observable substrate peaks in the SXPS, see Figure S1 in the ESI) film of TiOPc on Cu(1 1 1) are shown as a function of the incidence angle. Note that the signal in normal incidence is almost, but not entirely, suppressed for all spectra, indicating that the molecular macrocycle must be adsorbed almost parallel to the surface plane, even in thicker multilayer regimes.

adsorption height of the N atoms. The N atoms that bridge the isoindolic rings were kept fixed. Two potential molecular confirmations resulted from this search. The first model resembles that of a saddle shape distortion of the molecule, where two isoindolic rings were tilted away from the surface, and two towards the surface. The other model had smaller tilts of the isoindolic rings, but a more significant vertical offset, which we have labelled as the vertical offset model. These two models are shown schematically in Fig. 6, and their cartesian coordinates are listed in the ESI in Table S2.

The saddle shape model (Fig. 6a) has one pair of isoindolic rings tilted 14° away from the surface, the other pair tilted 10° down towards the surface. The inner N atoms are displaced by 0.8 Å, with respect to one another. The vertical offset model (Fig. 6b) has all four isoindolic rings tilted by less than 5° in each direction (with respect to the surface plane), but they are vertically offset by 0.5–0.7 Å, with respect to one another. The vertical offset model is broadly comparable to the DFT structure presented by Snezhakova et al. [26] and Jabrane et al. [20], however their calculations predicted a vertical offset of 0.06–0.20 Å. Both of these models would be compatible with the measured NEXAFS presented above, and the expected coherent fraction and coherent position for each model is listed in Table 1, alongside the experimental results.

A similar modelling for the TiOPc adsorption structure did not yield any structures that agreed well with the CN, CC and N results. Furthermore, even if a single-site model existed that yielded excellent agreement with the CN, CC and N results, such a model cannot explain the very low coherent fraction observed for the O atoms.

4. Discussion

Whereas a mild distortion in the phthalocyanine macrocycle can explain all of the experimental results published herein for FePc, this is not true for TiOPc. Indeed, like the previously published VOPc results on Cu(1 1 1) [16], it seems likely that the TiOPc molecule adsorbs with different orientations on the surface. Up to moderately thick multilayers, the TiOPc molecule is largely flat upon the surface, and one can expect these different orientations must all share an adsorption structure where the molecular macrocycle mostly parallel to co-adsorbed molecules and the surface. As the coherent fraction of the Ti atoms remains high, yet all other species exhibit a low coherent fraction, it is unlikely that the molecule at sub-monolayer coverages adsorbs in a continuum of different adsorption heights. However, a combination of configurations that differ primarily in the orientation of the Ti = O bond could explain all of the data presented here. Specifically, the occupation of two unique orientations, one where the O atom is more distant from the underlying surface than the Ti atom ("upwards pointing"), and one where the O atom is between the underlying surface and the Ti atom ("downwards pointing"), would qualitatively explain the TiOPc results. An example of such structures are shown schematically in Fig. 1c, and such a model was used to explain the previously published NIXSW VOPc results [16], as well as STM and non-contact atomic force microscopy (nc-AFM) measurements of TiOPc [47,75], on the Cu(1 1 1) surface and titanyl tetraphenyl porphyrin (TiOTPP) on TiO_2(1 1 0) [76]. Interestingly, this is counter to measurements of the same systems adsorbed on Au(1 1 1), where VOPc and TiOPc have been found to only adsorb in the "upwards" configuration. [35,77].

As discussed in the SXPS section, two peaks were observed in the O 1s data. Due to a low signal to noise ratio (see, for example, Figure S3 in the ESI), quantitatively assessing the NIXSW results of fitting these features independently is not reasonable, however a qualitative comparison of this fit is indicative and is shown in Fig. 7. While the spectra are noisy, there is clearly a stark difference between the two yield profiles. Indeed, the profile of O_1 species clearly has its maxima at a higher photon energy than the O_2 species. Such a difference indicates that the two different species occupy two different heights on the surface, which could obviously be related to the upwards and downwards pointing species. Note that this difference will primarily be due to a difference in coherent position: variations in coherent fraction primarily effect the size of the maximum photoelectron yield, but have only a minor effect on the position of that maxima. Importantly, differences in the position in photon energy of the maximum photoelectron yield are primarily due to differing coherent positions. Considering the adsorption height of the Ti centre, 3.0 ± 0.2 Å, and assuming a Ti = O bond length of 1.6 Å, the expected coherent positions for the two O atoms would be ~ 0.7 for the

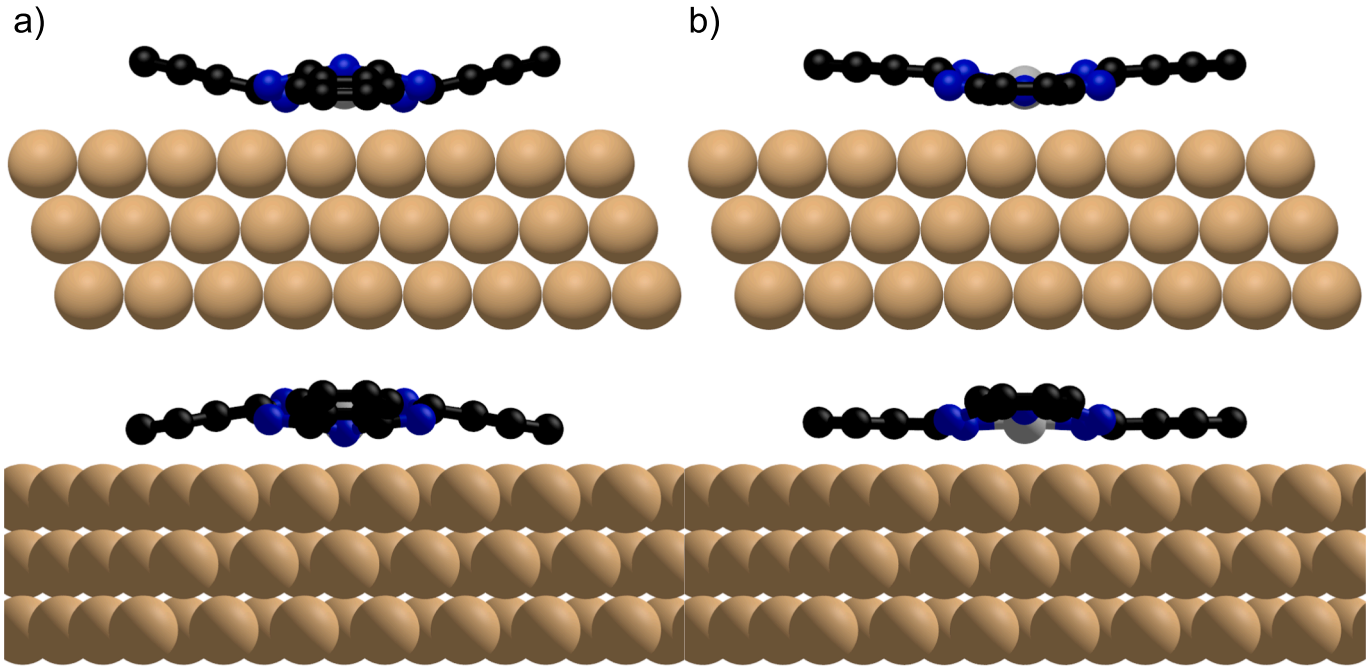

Fig. 6. Schematic of the (a) saddle shape and (b) vertical offset model of the FePc structure viewing along a (top) < 111 > and (bottom) < $2\overline{11}$ > direction. The associated coherent fraction and coherent position that would be expected from these models are listed in Table 1. Note that the Fe atom was fixed at an adsorption height of 2.44 Å, corresponding to a p_{111} of 1.17 in both models.

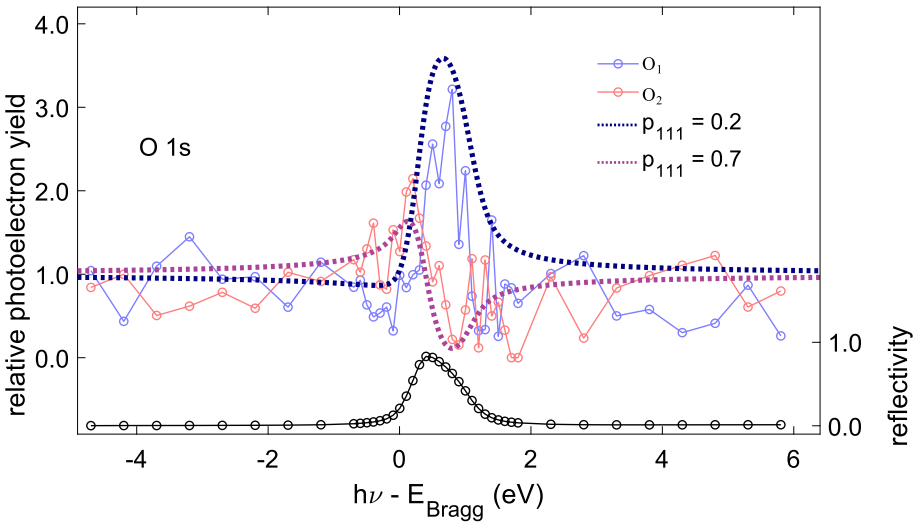

Fig. 7. The (111) O 1s NIXSW of a submonolayer of TiOPc on Cu(1 1 1) deconvoluted into two components, O_1 and O_2 observed in the SXPS (Fig. 2). Overlaid are the expected relative photoelectron yields for O atoms with a p_{111} of 0.2 and 0.7, corresponding to an adsorption height 1.6 Å below or above (respectively) the measured Ti height, 3.00 ± 0.20 Å.

downward pointing species and ~ 2.2/0.2 for the upwards pointing species. The expected yield profile for these two coherent positions, assuming a coherent fraction of 1.0, are overlaid in Fig. 7. While the experimental data is noisy, it is clear that a coherent position of around 0.2 for the O_1 species, and around 0.7 for the O_2 species would be reasonable.

The measured adsorption height of the Ti metal centre (3.00 ± 0.20 Å) is effectively identical to that previously measured for the V metal centre of VOPc on the same surface (3.05 ± 0.06 Å),[16] and indicates a weak interaction directly between the Ti metal centres and the underlying surface, even when the Ti atoms are closer to the surface than the O atoms. The adsorption height of the Fe metal centre (2.44 ± 0.09 Å), lies between that of the Zn metal centre for ZnPc (2.25 ± 0.05 Å) and fluorinated ZnPc (F_{16}ZnPc – 2.58 ± 0.05 Å)[78], where the metal centre is found to lie closer to the substrate, than the molecular macrocycle corresponding to significant overlap of the orbitals of the metal centre with the electronic bands of the substrate. We have observed no evidence of a surface reconstruction, as has previously been observed for FePc on Cu(1 1 0) [79], though a surface reconstruction induced by the downwards pointing TiOPc could help explain the comparatively low adsorption height (~1.4 Å) of the O atom for this species. The distortion observed for the FePc molecule here, was not observed for the adsorption of FePc on Ag(1 1 1) [37], where the measured coherent fractions for the CC, CN and N species were closer to unity. Coupled with the similar such structure determination for free-base tetraphenyl porphyrin on Cu(1 1 1) [19], which indicated a significant distortion of the molecular macrocycle upon adsorption, due to the strong interactions between the substrate and the central N atoms. These results when taken together suggest that the Cu substrate may be expected to distort tetrapyrroles and other pyrrolic macrocycles (e.g. corroles, subphthalocyanine, etc.) adsorbed to its surface.

5. Conclusions

We have performed SXPS, NIXSW and NEXAFS measurements of iron phthalocyanine (FePc) and titanyl phthalocyanine (TiOPc) adsorbed on Cu(1 1 1). We interpret the NEXAFS results as indicating that both molecules adsorb with the molecular macrocycle mostly parallel to the surface plane. The NIXSW results indicate that the FePc likely adsorbs in a single configuration, but with measurable deformation of the molecule, which could be reconciled with either a vertical offset of the isoindole groups or a saddle shape conformation. The NIXSW results for the TiOPc could not be reconciled with a single adsorption configuration, and rather point to the coexistence of at least two different configurations. One possible explanation would be a mixture of two configurations: one with the O atom between the Ti and the surface, and one with the Ti atom between the O atom and the surface, similar to what was previously proposed for VOPc on the same surface [16]. Separately fitting the two peaks present in the O 1s NIXSW measurements results in a photoelectron yield profile that could be explained by such a model. These results suggest a general trend that planar phthalocyanines adsorb in a single adsorption configuration on the Cu(1 1 1) surface, but that non-planar phthalocyanines adsorb in multiple adsorption configurations, which may have an impact on the patterning of thin films on Cu electrodes, as well as junctions formed between such films and electrodes.

Author contribution

M.A.S., B.P.K., M.C., L.B.S.W., P.F., D.C.G. and D.A.D. were involved in the acquisition of the data. D.A.D. analysed the data. D.A.D., M.A.S, L. A.R. and B.P.K. were involved in the experimental conceptualisation. D. A.D and A.S. were involved in the supervision of the project. D.A.D. and L.A.R. took primary responsibility for drafting the article. All authors contributed to the review and editing of the article.

Declaration of Competing Interest

The authors declare that they have no known competing financial interests or personal relationships that could have appeared to influence the work reported in this paper.

Data availability

Data will be made available on request.

Acknowledgements

The authors thank Diamond Light Source for access to beamline I09 (SI30875-1, NT31165-2 and NT31165-4) and to B07 (SI29418-1). B.P.K. acknowledges support from the DFG under the Walter Benjamin fellowship programme (KL 3430/1-1). M.A.S. acknowledges support from the Analytical Science CDT at the University of Warwick. M.C. acknowledges support via the MI&A Doctoral Training Programme at

the University of Nottingham (EPSRC). A.S. acknowledges support via a Royal Society University Research Fellowship.

Appendix A. Supplementary data

Supplementary data to this article can be found online at https://doi.org/10.1016/j.ica.2023.121679.

References

[1] G. Avvisati, P. Gargiani, C. Mariani, M.G. Betti, Tuning the Magnetic Coupling of a Molecular Spin Interface via Electron Doping, Nano Lett. 21 (2021) 666–672, https://doi.org/10.1021/ACS.NANOLETT.0C04256.

[2] L.M. Arruda, M. Ehesan Ali, M. Bernien, F. Nickel, J. Kopprasch, C. Czekelius, P. M. Oppeneer, W. Kuch, Modifying the Magnetic Anisotropy of an Iron Porphyrin Molecule by an on-Surface Ring-Closure Reaction, J. Phys. Chem. C 123 (2019) 14547–14555, https://doi.org/10.1021/acs.jpcc.9b03126.

[3] H. Wang, B.W. Wang, Y. Bian, S. Gao, J. Jiang, Single-molecule magnetism of tetrapyrrole lanthanide compounds with sandwich multiple-decker structures, Coord. Chem. Rev. 306 (2016) 195–216, https://doi.org/10.1016/J.CCR.2015.07.004.

[4] D. Tudor, I. Nenu, G.A. Filip, D. Olteanu, M. Cenariu, F. Tabaran, R.M. Ion, L. Gligor, I. Baldea, Combined regimen of photodynamic therapy mediated by Gallium phthalocyanine chloride and Metformin enhances anti-melanoma efficacy, PLoS One. 12 (2017) e0173241. https://doi.org/10.1371/journal.pone.0173241.

[5] Z. Jiang, J. Shao, T. Yang, J. Wang, L. Jia, Pharmaceutical development, composition and quantitative analysis of phthalocyanine as the photosensitizer for cancer photodynamic therapy, J. Pharm. Biomed. Anal. 87 (2014) 98–104, https://doi.org/10.1016/j.jpba.2013.05.014.

[6] Z. Wang (王正君), L.i. Pi, M.S. Seehra, J. Bindra, H. van Tol, N.S. Dalal, Magnetic studies reveal near-perfect paramagnetism in the molecular semiconductor vanadyl phthalocyanine (C32H16N8VO), J. Magn. Magn. Mater. 422 (2017) 386–390.

[7] M. Atzori, L. Tesi, E. Morra, M. Chiesa, L. Sorace, R. Sessoli, Room-Temperature Quantum Coherence and Rabi Oscillations in Vanadyl Phthalocyanine: Toward Multifunctional Molecular Spin Qubits, J. Am. Chem. Soc. 138 (7) (2016) 2154–2157.

[8] J.M. Robertson, I. Woodward, Crystal structure of β-copper phthalocyanine, J. Chem. Soc. A (1968) 2488–2493, https://doi.org/10.1039/J19680002488.

[9] A.J. Ramadan, L.A. Rochford, D.S. Keeble, P. Sullivan, M.P. Ryan, T.S. Jones, S. Heutz, Exploring high temperature templating in non-planar phthalocyanine/copper iodide (111) bilayers, J Mater Chem C Mater. 3 (2014) 461–465, https://doi.org/10.1039/C4TC02116A.

[10] G. de la Torre, P. Vázquez, F. Agulló-López, T. Torres, Role of structural factors in the nonlinear optical properties of phthalocyanines and related compounds, Chem. Rev. 104 (2004) 3723–3750, https://doi.org/10.1021/CR030206T.

[11] C.G. Claessens, U. Hahn, T. Torres, Phthalocyanines: From outstanding electronic properties to emerging applications, Chem. Rec. 8 (2008) 75–97, https://doi.org/10.1002/TCR.20139.

[12] T. Furuyama, K. Satoh, T. Kushiya, N. Kobayashi, Design, synthesis, and properties of phthalocyanine complexes with main-group elements showing main absorption and fluorescence beyond 1000 nm, J Am Chem Soc. 136 (2014) 765–776, https://doi.org/10.1021/JA411016F/SUPPL_FILE/JA411016F_SI_007.CIF.

[13] L. Keith Woo, J. Alan Hays, R.A. Jacobson, C.L. Day, Low-Valent Titanium Porphyrin Complexes: Synthesis and Structural Characterization of the First Titanium(II) Porphyrin Complex, (η2-Dlphenylacetylene)titanium Octaethylporphyrin, Organometallics 10 (1991) 2102–2104, https://doi.org/10.1021/OM00053A009.

[14] A.J. Ramadan, S. Fearn, T.S. Jones, S. Heutz, L.A. Rochford, Film formation of non-planar phthalocyanines on copper(I) iodide, RSC Adv. 6 (2016) 95227–95231, https://doi.org/10.1039/C6RA21803B.

[15] E. Wruss, O.T. Hofmann, D.A. Egger, E. Verwüster, A. Gerlach, F. Schreiber, E. Zojer, Adsorption Behavior of Nonplanar Phthalocyanines: Competition of Different Adsorption Conformations, J. Phys. Chem. C 120 (2016) 6869–6875, https://doi.org/10.1021/acs.jpcc.6b00312.

[16] P.J. Blowey, R.J. Maurer, L.A. Rochford, D.A. Duncan, J.H. Kang, D.A. Warr, A. J. Ramadan, T.L. Lee, P.K. Thakur, G. Costantini, K. Reuter, D.P. Woodruff, The Structure of VOPc on Cu(111): Does V=O Point Up, or Down, or Both? J. Phys. Chem. C 123 (2019) 8101–8111, https://doi.org/10.1021/ACS.JPCC.8B07530/.

[17] B.P. Rand, D. Cheyns, K. Vasseur, N.C. Giebink, S. Mothy, Y. Yi, V. Coropceanu, D. Beljonne, J. Cornil, J.L. Brédas, J. Genoe, The Impact of Molecular Orientation on the Photovoltaic Properties of a Phthalocyanine/Fullerene Heterojunction, Adv. Funct. Mater. 22 (2012) 2987–2995, https://doi.org/10.1002/ADFM.201200512.

[18] J.M. Gottfried, Surface chemistry of porphyrins and phthalocyanines, Surf. Sci. Rep. 70 (2015) 259–379, https://doi.org/10.1016/J.SURFREP.2015.04.001.

[19] P.T.P. Ryan, P.L. Lalaguna, F. Haag, P.L. Lalaguna, P. Ding, M.M. Braim, J.V. Barth, T.L. Lee, D.P. Woodruff, F. Allegretti, D.A. Duncan, Validation of the inverted adsorption structure for free-base tetraphenyl porphyrin on Cu(111), Chem. Commun. 56 (2020) 3681–3684, https://doi.org/10.1039/C9CC09638H.

[20] M. Jabrane, M. El Hafidi, M.Y. El Hafidi, A. Kara, Fe-Phthalocyanine on Cu(111) and Ag(111): A DFT+vdWs investigation, Surf. Sci. 716 (2022), 121961, https://doi.org/10.1016/J.SUSC.2021.121961.

[21] K. Greulich, A. Belser, T. Basova, T. Chassé, H. Peisert, Interfaces between Different Iron Phthalocyanines and Au(111): Influence of the Fluorination on Structure and Interfacial Interactions, J. Phys. Chem. C 126 (2022) 716–727, https://doi.org/10.1021/ACS.JPCC.1C08826.

[22] R. Žitko, G.G. Blesio, L.O. Manuel, A.A. Aligia, Iron phthalocyanine on Au(111) is a "non-Landau" Fermi liquid, Nature Communications 2021 12:1. 12 (2021) 1–9. https://doi.org/10.1038/s41467-021-26339-z.

[23] J. Granet, M. Sicot, I.C. Gerber, G. Kremer, T. Pierron, B. Kierren, L. Moreau, Y. Fagot-Revurat, S. Lamare, F. Chérioux, D. Malterre, Adsorption-Induced Kondo Effect in Metal-Free Phthalocyanine on Ag(111), J. Phys. Chem. C 124 (2020) 10441–10452, https://doi.org/10.1021/ACS.JPCC.9B11141.

[24] A.C. Papageorgiou, P. Knecht, P.T.P. Ryan, D.A. Duncan, L. Jiang, J. Reichert, P. S. Deimel, F. Haag, J.T. Küchle, F. Allegretti, T.L. Lee, M. Schwarz, M. Garnica, W. Auwärter, A.P. Seitsonen, J.V. Barth, Tunable interface of ruthenium porphyrins and silver, J. Phys. Chem. C 125 (2021) 3215–3224, https://doi.org/10.1021/ACS.JPCC.0C10418.

[25] R.C. De Campos Ferreira, A. Pérez Paz, D.J. Mowbray, J.Y. Roulet, R. Landers, A., De Siervo, Supramolecular Ordering and Reactions of a Chlorophenyl Porphyrin on Ag(111), J. Phys. Chem. C 124 (2020) 14220–14228, https://doi.org/10.1021/ACS.JPCC.0C02953.

[26] O. Snezhkova, J. Lüder, A. Wiengarten, S.R. Burema, F. Bischoff, Y. He, J. Rusz, J. Knudsen, M.-L. Bocquet, K. Seufert, J.V. Barth, W. Auwärter, B. Brena, J. Schnadt, Nature of the bias-dependent symmetry reduction of iron phthalocyanine on Cu(111), Phys. Rev. B 92 (2015) 75428, https://doi.org/10.1103/PhysRevB.92.075428.

[27] D.A. Duncan, P.S. Deimel, A. Wiengarten, R. Han, R.G. Acres, W. Auwärter, P. Feulner, A.C. Papageorgiou, F. Allegretti, J.V. Barth, Immobilised molecular catalysts and the role of the supporting metal substrate, Chem. Commun. 51 (2015) 9483–9486, https://doi.org/10.1039/C5CC01639H.

[28] F. Petraki, H. Peisert, U. Aygül, F. Latteyer, J. Uihlein, A. Vollmer, T. Chassé, Electronic structure of FePc and interface properties on Ag(111) and Au(100), J. Phys. Chem. C 116 (2012) 11110–11116, https://doi.org/10.1021/JP302233E.

[29] A. Belser, K. Greulich, P. Nagel, M. Merz, S. Schuppler, T. Chassé, H. Peisert, Interface Properties of Perfluorinated Iron Phthalocyanine on Au(111) and Ag (111): The Influence of Iron and the Macrocycle, J. Phys. Chem. C 126 (2022) 14245–14254, https://doi.org/10.1021/ACS.JPCC.2C02694/.

[30] M. Fanetti, A. Calzolari, P. Vilmercati, C. Castellarin-Cudia, P. Borghetti, G. Di Santo, L. Floreano, A. Verdini, A. Cossaro, I. Vobornik, E. Annese, F. Bondino, S. Fabris, A. Goldoni, Structure and molecule - Substrate interaction in a Co-octaethyl porphyrin monolayer on the Ag(110) surface, J. Phys. Chem. C 115 (2011) 11560–11568, https://doi.org/10.1021/JP2011233/.

[31] D.A. Duncan, P.S. Deimel, A. Wiengarten, M. Paszkiewicz, P. Casado Aguilar, R. G. Acres, F. Klappenberger, W. Auwärter, A.P. Seitsonen, J.V. Barth, F. Allegretti, Bottom-Up fabrication of a metal-supported oxo-metal porphyrin, J. Phys. Chem. C 123 (2019) 31011–31025, https://doi.org/10.1021/ACS.JPCC.9B08661.

[32] W. Auwärter, K. Seufert, F. Klappenberger, J. Reichert, A. Weber-Bargioni, A. Verdini, D. Cvetko, M. Dell'Angela, L. Floreano, A. Cossaro, G. Bavdek, A. Morgante, A.P. Seitsonen, J.V. Barth, Site-specific electronic and geometric interface structure of Co-tetraphenyl-porphyrin layers on Ag(111), Phys. Rev. B: Condens. Matter Mater. Phys. 81 (2010), 245403, https://doi.org/10.1103/PHYSREVB.81.245403.

[33] A.C. Papageorgiou, K. Diller, S. Fischer, F. Allegretti, F. Klappenberger, S.C. Oh, Ö. Sağlam, J. Reichert, A. Wiengarten, K. Seufert, W. Auwärter, J.V. Barth, In Vacuo Porphyrin Metalation on Ag(111) via Chemical Vapor Deposition of Ru3(CO)12: Mechanistic Insights, J. Phys. Chem. C 120 (2016) 8751–8758, https://doi.org/10.1021/ACS.JPCC.6B01457.

[34] P. Knecht, D. Meier, J. Reichert, D.A. Duncan, M. Schwarz, J.T. Küchle, T.-L. Lee, P. S. Deimel, P. Feulner, F. Allegretti, W. Auwärter, G. Médard, A.P. Seitsonen, J. V. Barth, A.C. Papageorgiou, N-Heterocyclic Carbenes: Molecular Porters of Surface Mounted Ru-Porphyrins, Angew. Chem. 134 (2022) e202211877.

[35] D.A. Duncan, W. Unterberger, K.A. Hogan, T.J. Lerotholi, C.L.A. Lamont, D. P. Woodruff, A photoelectron diffraction investigation of vanadyl phthalocyanine on Au(1 1 1), Surf. Sci. 604 (2010) 47–53, https://doi.org/10.1016/J.SUSC.2009.10.018.

[36] I. Kröger, B. Stadtmüller, C. Kleimann, P. Rajput, C. Kumpf, Normal-incidence x-ray standing-wave study of copper phthalocyanine submonolayers on Cu(111) and Au(111), Phys. Rev. B 83 (2011), 195414, https://doi.org/10.1103/PhysRevB.83.195414.

[37] P.S. Deimel, R.M. Bababrik, B. Wang, P.J. Blowey, L.A. Rochford, P.K. Thakur, T. L. Lee, M.L. Bocquet, J.V. Barth, D.P. Woodruff, D.A. Duncan, F. Allegretti, Direct quantitative identification of the "surface trans -effect", Chem. Sci. 7 (2016) 5647–5656, https://doi.org/10.1039/C6SC01677D.

[38] D.A. Duncan, P. Casado Aguilar, M. Paszkiewicz, K. Diller, F. Bondino, E. Magnano, F. Klappenberger, I. Píš, A. Rubio, J. V. Barth, A. Pérez Paz, F. Allegretti, Local adsorption structure and bonding of porphine on Cu(111) before and after self-metalation, J Chem Phys. 150 (2019) 094702. https://doi.org/10.1063/1.5084027.

[39] A. Gerlach, F. Schreiber, S. Sellner, H. Dosch, I.A. Vartanyants, B.C.C. Cowie, T. L. Lee, J. Zegenhagen, Adsorption-induced distortion of F16 CuPc on Cu(111) and Ag(111): An x-ray standing wave study, Phys. Rev. B: Condens. Matter Mater. Phys. 71 (2005), 205425, https://doi.org/10.1103/PHYSREVB.71.205425.

[40] I. Kröger, B. Stadtmüller, C. Stadler, J. Ziroff, M. Kochler, A. Stahl, F. Pollinger, T. L. Lee, J. Zegenhagen, F. Reinert, C. Kumpf, Submonolayer growth of copper-phthalocyanine on Ag(111), New J. Phys. 12 (2010), 083038, https://doi.org/10.1088/1367-2630/12/8/083038.

[41] C. Stadler, S. Hansen, F. Pollinger, C. Kumpf, E. Umbach, T.L. Lee, J. Zegenhagen, Structural investigation of the adsorption of SnPc on Ag(111) using normal-

incidence x-ray standing waves, Phys. Rev. B: Condens. Matter Mater. Phys. 74 (2006), 035404, https://doi.org/10.1103/PHYSREVB.74.035404.
[42] A. Gerlach, T. Hosokai, S. Duhm, S. Kera, O.T. Hofmann, E. Zojer, J. Zegenhagen, F. Schreiber, Orientational Ordering of Nonplanar Phthalocyanines on Cu(111): Strength and Orientation of the Electric Dipole Moment, Phys. Rev. Lett. 106 (2011), 156102, https://doi.org/10.1103/PhysRevLett.106.156102.
[43] J.D. Baran, J.A. Larsson, R.A.J. Woolley, Y. Cong, P.J. Moriarty, A.A. Cafolla, K. Schulte, V.R. Dhanak, Theoretical and experimental comparison of SnPc, PbPc, and CoPc adsorption on Ag(111), Phys. Rev. B: Condens. Matter Mater. Phys. 81 (2010), 075413, https://doi.org/10.1103/PHYSREVB.81.075413.
[44] M. Lepper, J. Köbl, T. Schmitt, M. Gurrath, A. De Siervo, M.A. Schneider, H. P. Steinrück, B. Meyer, H. Marbach, W. Hieringer, "Inverted" porphyrins: a distorted adsorption geometry of free-base porphyrins on Cu(111), Chem. Commun. 53 (2017) 8207–8210, https://doi.org/10.1039/C7CC04182A.
[45] W. Auwärter, F. Klappenberger, A. Weber-Bargioni, A. Schiffrin, T. Strunskus, C. Wöll, Y. Pennec, A. Riemann, J.V. Barth, Conformational adaptation and selective adatom capturing of tetrapyridyl-porphyrin molecules on a copper (111) surface, J. Am. Chem. Soc. 129 (2007) 11279–11285, https://doi.org/10.1021/JA071572N.
[46] T. Niu, M. Zhou, J. Zhang, Y. Feng, W. Chen, Dipole Orientation Dependent Symmetry Reduction of Chloroaluminum Phthalocyanine on Cu(111), J. Phys. Chem. C 117 (2013) 1013–1019, https://doi.org/10.1021/jp310196k.
[47] W. Zhao, H. Zhu, H. Song, J. Liu, Q. Chen, Y. Wang, K. Wu, Adsorption and Assembly of Photoelectronic TiOPc Molecules on Coinage Metal Surfaces, J. Phys. Chem. C 122 (2018) 7695–7701, https://doi.org/10.1021/ACS.JPCC.7B12673.
[48] D.P. Woodruff, Surface structure determination using x-ray standing waves, Rep. Prog. Phys. 68 (2005) 743–798, https://doi.org/10.1088/0034-4885/68/4/R01.
[49] O. Snezhkova, F. Bischoff, Y. He, A. Wiengarten, S. Chaudhary, N. Johansson, K. Schulte, J. Knudsen, J. V. Barth, K. Seufert, W. Auwärter, J. Schnadt, Iron phthalocyanine on Cu(111): Coverage-dependent assembly and symmetry breaking, temperature-induced homocoupling, and modification of the adsorbate-surface interaction by annealing , J. Chem. Phys. 144 (2016) 94702. https://doi.org/10.1063/1.4942121.
[50] Y. Wei, J.E. Reutt-Robey, Directed organization of C70 kagome lattice by titanyl phthalocyanine monolayer template, J. Am. Chem. Soc. 133 (2011) 15232–15235, https://doi.org/10.1021/JA206175C.
[51] L.A. Rochford, D.S. Keeble, O.J. Holmes, G.J. Clarkson, T.S. Jones, Controlling templating effects at the organic/inorganic interface using (111) oriented copper iodide †, J Mater Chem C Mater. 2 (30) (2014) 6056–6060.
[52] T.L. Lee, D.A. Duncan, A Two-Color Beamline for Electron Spectroscopies at Diamond Light Source, Synchrotron Radiat News. 31 (2018) 16–22, https://doi.org/10.1080/08940886.2018.1483653.
[53] C.J. Fisher, R. Ithin, R.G. Jones, G.J. Jackson, D.P. Woodruff, B.C.C. Cowie, Non-dipole photoemission effects in x-ray standing wavefield determination of surface structure, Journal of Physics: Condensed Matter. 10 (1998) L623. https://doi.org/10.1088/0953-8984/10/35/004.
[54] V.I. Nefedov, V.G. Yarzhemsky, I.S. Nefedova, M.B. Trzhaskovskaya, I.M. Band, The influence of non-dipolar transitions on the angular photoelectron distribution, J Electron Spectros Relat Phenomena. 107 (2000) 123–130, https://doi.org/10.1016/S0368-2048(00)00094-3.
[55] S. Doniach, M. Sunjic, Many-electron singularity in X-ray photoemission and X-ray line spectra from metals, J. Phys. C Solid State Phys. 3 (2) (1970) 285–291.
[56] D.C. Grinter, F. Venturini, P. Ferrer, M.A. van Spronsen, R. Arrigo, W. Quevedo Garzon, K. Roy, A.I. Large, S. Kumar, G. Held, The Versatile Soft X-Ray (VerSoX) Beamline at Diamond Light Source, Synchrotron Radiat News. 35 (2022) 39–47, https://doi.org/10.1080/08940886.2022.2082181.
[57] G. Held, F. Venturini, D.C. Grinter, P. Ferrer, R. Arrigo, L. Deacon, W.Q. Garzon, K. Roy, A. Large, C. Stephens, A. Watts, P. Larkin, M. Hand, H. Wang, L. Pratt, J. J. Mudd, T. Richardson, S. Patel, M. Hillman, S. Scott, Ambient-pressure endstation of the Versatile Soft X-ray (VerSoX) beamline at Diamond Light Source, J. Synchrotron Radiat. 27 (2020) 1153–1166, https://doi.org/10.1107/S1600577520009157/VE5129SUP1.PDF.
[58] J. Stöhr, H. König, Determination of Spin- and Orbital-Moment Anisotropies in Transition Metals by Angle-Dependent X-Ray Magnetic Circular Dichroism, Phys. Rev. Lett. 75 (20) (1995) 3748–3751.
[59] B. Stadtmüller, M. Gruenewald, J. Peuker, R. Forker, T. Fritz, C. Kumpf, Molecular Exchange in a Heteromolecular PTCDA/CuPc Bilayer Film on Ag(111), J. Phys. Chem. C 118 (2014) 28592–28602, https://doi.org/10.1021/jp5078104.
[60] C. Isvoranu, J. Knudsen, E. Ataman, K. Schulte, B. Wang, M.L. Bocquet, J. N. Andersen, J. Schnadt, Adsorption of ammonia on multilayer iron phthalocyanine, J. Chem. Phys. 134 (2011), https://doi.org/10.1063/1.3563636/71902.
[61] C. Isvoranu, B. Wang, K. Schulte, E. Ataman, J. Knudsen, J.N. Andersen, M.L. Bocquet, J. Schnadt, Tuning the spin state of iron phthalocyanine by ligand adsorption, Journal of Physics: Condensed Matter. 22 (2010) 472002. https://doi.org/10.1088/0953-8984/22/47/472002.
[62] M.J. Bedzyk, G. Materlik, Two-beam dynamical diffraction solution of the phase problem: A determination with x-ray standing-wave fields, Phys. Rev. B 32 (1985) 6456–6463, https://doi.org/10.1103/PhysRevB.32.6456.
[63] B.W. Batterman, Effect of dynamical diffraction in x-ray fluorescence scattering, Physical Review. 133 (1964) A759–A764. https://doi.org/10.1103/PhysRev.133.A759.
[64] J. Zegenhagen, A. Kaimirov, The X-Ray Standing Wave Technique, in: 2013: pp. 3–35.
[65] D.P. Woodruff, D.A. Duncan, X-ray standing wave studies of molecular adsorption: why coherent fractions matter, New J Phys. 22 (2020) 113012. https://doi.org/10.1088/1367-2630/ABC63A.
[66] J.F. Kirner, W. Dow, W.R. Scheidt, Molecular Stereochemistry of Two Intermediate-Spin Complexes. Iron(II) Phthalocyanine and Manganese(II) Phthalocyanine, Inorg. Chem. 15 (1976) 1685–1690, https://doi.org/10.1021/IC50161A042.
[67] M. Schwarz, M. Garnica, D.A. Duncan, A. Pérez, P. Paz, J. Ducke, P.S. Deimel, P. K. Thakur, T.-L. Lee, A. Rubio, J.V. Barth, F. Allegretti, W. Auwa ̈ Rter,, Adsorption Conformation and Lateral Registry of Cobalt Porphine on Cu(111), J. Phys. Chem. C. 122 (2018) 34, https://doi.org/10.1021/acs.jpcc.7b11705.
[68] A. Baklanov, J.T. Küchle, D.A. Duncan, P.T.P. Ryan, R.J. Maurer, M. Schwarz, E. Corral Rascon, I. Piquero-Zulaica, T.H. Ngo, A. Riss, F. Allegretti, W. Auwärter, Zinc-Porphine on Coinage Metal Surfaces: Adsorption Configuration and Ligand-induced Central Atom Displacement, The Journal of Physical Chemistry C. under review (n.d.).
[69] A. Scarfato, S.H. Chang, S. Kuck, J. Brede, G. Hoffmann, R. Wiesendanger, Scanning tunneling microscope study of iron(II) phthalocyanine growth on metals and insulating surfaces, Surf. Sci. 602 (2008) 677–683, https://doi.org/10.1016/J.SUSC.2007.11.011.
[70] K. Diller, R.J. Maurer, M. Müller, K. Reuter, Interpretation of x-ray absorption spectroscopy in the presence of surface hybridization, J Chem Phys. 146 (2017) 214701. https://doi.org/10.1063/1.4984072.
[71] Y. Wei, S.W. Robey, J.E. Reutt-Robey, Flux-Selected Titanyl Phthalocyanine Monolayer Architecture on Ag (111), J. Phys. Chem. C 112 (47) (2008) 18537–18542.
[72] M. Polek, F. Latteyer, T.V. Basova, F. Petraki, U. Aygül, J. Uihlein, P. Nagel, M. Merz, S. Schuppler, T. Chassé, H. Peisert, Chemical reaction of polar phthalocyanines on silver: Chloroaluminum phthalocyanine and fluoroaluminum phthalocyanine, J. Phys. Chem. C 120 (2016) 24715–24723, https://doi.org/10.1021/ACS.JPCC.6B07052.
[73] K. Greulich, A. Belser, S. Bölke, P. Grüninger, R. Karstens, M.S. Sättele, R. Ovsyannikov, E. Giangrisostomi, T.V. Basova, D. Klyamer, T. Chassé, H. Peisert, Charge Transfer from Organic Molecules to Molybdenum Disulfide: Influence of the Fluorination of Iron Phthalocyanine, J. Phys. Chem. C 124 (2020) 16990–16999, https://doi.org/10.1021/ACS.JPCC.0C03862.
[74] K. Seufert, M.-L. Bocquet, W. Auwärter, A. Weber-Bargioni, J. Reichert, N. Lorente, J.V. Barth, Cis-dicarbonyl binding at cobalt and iron porphyrins with saddle-shape conformation, Nature Chem 3 (2) (2011) 114–119.
[75] B.K. Yuan, P.C. Chen, J. Zhang, Z.H. Cheng, X.H. Qiu, C. Wang, Orientation of molecular interface dipole on metal surface investigated by noncontact atomic force microscopy, Chin. Sci. Bull. 58 (2013) 3630–3635, https://doi.org/10.1007/S11434-013-5977-X/METRICS.
[76] L. Schio, D. Forrer, M. Casarin, A. Goldoni, C. Rogero, A. Vittadini, L. Floreano, On surface chemical reactions of free-base and titanyl porphyrins with r-TiO 2 (110): a unified picture, PCCP 24 (2022) 12719–12744, https://doi.org/10.1039/D2CP01073A.
[77] S.C.B. Mannsfeld, T. Fritz, Understanding organic-inorganic heteroepitaxial growth of molecules on crystalline substrates: Experiment and theory, Phys. Rev. B: Condens. Matter Mater. Phys. 71 (2005), 235405, https://doi.org/10.1103/PHYSREVB.71.235405/FIGURES/8/MEDIUM.
[78] H. Yamane, A. Gerlach, S. Duhm, Y. Tanaka, T. Hosokai, Y.Y. Mi, J. Zegenhagen, N. Koch, K. Seki, F. Schreiber, Site-specific geometric and electronic relaxations at organic-metal interfaces, Phys. Rev. Lett. 105 (2010), 046103, https://doi.org/10.1103/PHYSREVLETT.105.046103.
[79] M. Abadía, R. González-Moreno, A. Sarasola, G. Otero-Irurueta, A. Verdini, L. Floreano, A. Garcia-Lekue, C. Rogero, Massive surface reshaping mediated by metal-organic complexes, J. Phys. Chem. C 118 (2014) 29704–29712, https://doi.org/10.1021/JP505802H/SUPPL_FILE/JP505802H_SI_001.PDF.